IEEE Access
Multidisciplinary | Rapid Review | Open Access Journal

Received June 12, 2019, accepted June 18, 2019, date of publication June 24, 2019, date of current version July 15, 2019.

Digital Object Identifier 10.1109/ACCESS.2019.2924435

Tracking Control via Iterative Learning for High-Speed Trains With Distributed Input Constraints

YONG CHEN, DEQING HUANG, (Member, IEEE), TENGFEI HUANG, AND NA QIN, (Member, IEEE)
School of Electrical Engineering, Southwest Jiaotong University, Chengdu 610031, China

Corresponding author: Na Qin (qinna@home.swjtu.edu.cn)

This work was supported in part by the National Natural Science Foundation of China under Grant 61773323, Grant 61433011, Grant 61603316, and Grant 61733015, in part by the Fundamental Research Funds for the Central Universities under Grant 2682018CX15, and in part by the Sichuan Science and Technology Program under Grant 2019YFG0345 and Grant 2019YJ0210.

ABSTRACT This paper investigates the tracking control problem of high-speed trains in the presence of the input constraints caused by the distribution and output capacity of power systems. By virtue of the repetitive operation pattern of trains and the backstepping technique, an adaptive iterative learning control (ILC) strategy based on the multi-particle model is proposed to drive the train to track the given reference displacement and velocity, where the unknown time-varying parameters are learned and adjusted between successive operations, and an input-dependent auxiliary system is introduced to compensate the influence of input constraints. During the design of the controller, the Lyapunov function and composite energy function (CEF) are constructed to ensure the stability of the closed-loop system and the convergence of tracking errors for high-speed trains. Furthermore, numerical simulation is performed to confirm the effectiveness of the proposed scheme. The three main contributions of this work lie in: 1) Integrating the multi-particle model and ILC framework, which can more accurately reveal the dynamics of the train, and take full advantage of the repetitive operation pattern; 2) Following the backstepping procedure to devise the learning controller, where the parameter uncertainties and modeling inaccuracies are deliberately handled, and; 3) Solving the issues of distributed input constraints for the control system of high-speed trains.

INDEX TERMS High-speed train, tracking control, distributed input constraints, iterative learning control, backstepping technique.

I. INTRODUCTION

As a momentous transportation tool, high-speed trains, characterized by the great technical difficulty and the complicated engineering etc., are the concentrate embodiment of modern science and technology. Among all the pivotal components, the automatic train operation (ATO) system, which can drive the trains to run automatically and stop accurately, is one of the core parts of automatic train control (ATC) system. Concretely, the main task of the ATO system is to regulate online the running states of high-speed trains according to the reference trajectories given in the scheduling plans, which are developed by the railway department aiming to compromise optimally between trip time and energy consumption of trains on the premise of ensuring the safety of trains [1]–[3]. Nevertheless, due to the limitations of distribution and output capacity of the power systems, the train control system is inevitably subject to the input constraints, which will easily cause the instability of control system, and even lead to the unsafety of the train operation in serious cases. To settle the tough issues, this paper will focus on the design of the tracking controller for high-speed trains in the presence of distributed input constraints.

By virtue of the intelligent control technology, the tracking control of high-speed train has been intensively studied so far. To name a few, [4] developed a tracking controller for

The associate editor coordinating the review of this manuscript and approving it for publication was Dong Shen.

high-speed trains with unknown parameters and nonlinear lumps to achieve the asymptotic convergence and disturbance rejection based on the robust adaptive control. In [5], a robust H_∞ controller is proposed for high-speed trains based on the multi-particle model, where unknown nonlinearities, parameters uncertainties and time-varying delays are considered together. Later, a robust adaptive nonsingular terminal sliding mode control strategy is integrated to handle the tracking control problem of position and velocity for the high-speed trains subjected to unknown parameters, model uncertainties, and external disturbances in [6]. Specially, a passivity-based control scheme, which is different from the Lyapunov-based method, is presented to realize the cruise control of train in [7]. Besides, more achievements with respect to the tracking control problems of high-speed trains can be found in [8]–[10]. Although these efforts have delivered some results, the stability of train control system with input constraints has not been investigated in the works mentioned above.

High-speed train is generally composed of two or more cars (motor cars) with power system and several cars (trailers) that do not own the traction force, where the motor car could provide the traction/braking force with the finite scope on account of the limitation of power systems, and the trailer can only supply the restricted braking force. Hence, it is of great practical significance to study the train control system with distributed input constraints, and the related researches have drawn some attention. Reference [11] proposed an adaptive state feedback controller for the high-speed trains with unknown parameters and nonlinearities to address the issues of unknown actuator failures and control input saturation. By integrating the sliding mode control and adaptive neural network technique, [12] solved the problem of the asymmetric nonlinear input saturation and thus achieve the tracking control of velocity and position of high-speed train. In [13], a hybrid model predictive controller is devised for high-speed trains to settle the automatic cruising control problem integrating the aim of tracking the reference speed and minimizing the energy consumption, where the nonlinear constraints of traction/braking forces are well considered. Furthermore, under the condition that the input suffers the saturation constraints, [14], [15] discussed the automatic control problem of trains based on the single particle model, and [16] investigated the coordinated control of multiple high-speed trains.

According to the scheduling plans, the high-speed train runs on the same railway periodically, e.g., the same tunnels, slopes and bridges, etc. Considering the repetitive pattern and the identical tracking target, the tracking control performance of train could be enhanced via iterative learning method, which can fully utilize the tracking error and control input information in the previous operation (iteration) to design the controller of current operation [17]–[27]. For instance, in [28], iterative learning control (ILC) algorithm is introduced into the automatic train supervision system to keep the running state of train consistent with the given reference trajectory. [29] further considered the cases of speed constraints and iteration-varying parameters. Reference [30] applied the terminal ILC method to the station stop control of train for the first time, and [31] tackled the overspeed protection of train via the coordinate ILC. All efforts are a good demonstration for the application of ILC in ATO system.

Attributing to the ubiquity in physical systems, the control systems with input constraints have long caught the attention of ILC community. Reference [32] coped with the input saturations for a class of nonlinear uncertain system under the ILC framework, where the controller included only a basic P-type feedback term. Reference [33] discussed the adaptive iterative learning reliable control for first-order nonlinear system with state delays and input saturation together. In [34], the design of adaptive ILC controller is investigated for the high-order systems with both state and input constraints, but the definition of error must resort to the Hurwitz polynomial. Recently, the command filtered adaptive backstepping technique is employed to devise the learning controller for high-order system in [35], where an auxiliary system is established to overcome the issues of input constraints. In terms of application, ILC is utilized to perform the speed tracking control for high-speed trains under the configurations of actuator failures, time-varying speed delays, and control input saturations in [36]. Later, an adaptive ILC scheme is proposed in [37] to realize the speed tracking for high-speed trains in the presence of unknown speed delays and input saturations. Unfortunately, similar to [28]–[31], [36] and [37] are also based on the single particle model, which treats the train as a single mass point and might not be applicable for practical train operation control.

In this paper, the tracking controller is devised for high-speed trains to follow the given displacement and velocity profiles via the iterative learning method and backstepping technique, where the multi-particle model with distributed input constraints is employed to describe the dynamics of train. The proposed controller is mainly composed of two parts: parameter adaptation and iterative learning, in which the adaptive term is used to estimate the unknown parameters, and the iterative learning term will take fully advantage of the repetitive pattern of train operation. During the design of controller, an auxiliary system with respect to the difference between the actual control input and the unsaturated input is introduced to ensure that all signals of control system are bounded, and the composite energy function (CEF) is constructed to analyze the stability of control system. Compared with the existing works, the main contributions of our paper include: 1) There is a little work to integrate the ILC method with the multi-particle model, which can characterize the dynamics of train more accurately, to achieve the tracking control of displacement and velocity for high-speed trains at present. 2) Since the model of train is formalized into a class of second-order system, the backstepping technique is adopted to facilitate the design of learning controller, where the unknown time-varying parameters and modeling inaccuracies are deliberately handled. 3) Taking fully into account the distribution and output capacity of power systems, the influence of input constraints on the stability of closed-loop control system is compensated through constructing an input-dependent auxiliary system.

This paper is organized as follows. In Section II, the dynamic model of high-speed train with input constraints is reviewed, and the control object is defined under the ILC framework. In Section III, an adaptive ILC controller is designed to track the given reference profiles for high-speed trains, and the stability of system is analyzed by constructing the CEF. Section IV confirms the effectiveness of the proposed scheme via numerical simulations. Section V concludes this work.

Notations: $\mathbb{R}^n$ and $\mathbb{R}^{n\times m}$ denote the sets of n-dimensional real vectors and $n \times m$ real matrixes respectively. $\|\cdot\|$ represents Euclidean norm of vectors, i.e., given a vector $\boldsymbol{x} = [x_1, x_2, \ldots, x_n]^T \in \mathbb{R}^n$, $\|\boldsymbol{x}\|^2 = \boldsymbol{x}^T\boldsymbol{x} = \sum_{j=1}^{n} x_j^2$. $\mathrm{tr}(\cdot)$ denotes the sum of the elements on the main diagonal of square matrix. $\mathrm{sat}(\cdot)$ is the saturation operator, which will be defined later. Specially, in our paper, when the arguments of $\mathrm{sat}(\cdot)$ are vectors or matrixes, the operations are performed component-wisely on each element. Moreover, let $\mathcal{D}(\cdot)$ denote the diag$(\cdot)$ function which returns a square diagonal matrix with the elements of vector, for the convenience of writing.

II. PRELIMINARIES

In this section, the preparatory works are introduced in detail, including the multi-particle model of high-speed trains with distributed input constraints, as well as the problem formulation for the displacement and velocity tracking control of high-speed trains under the ILC framework. Meanwhile, some necessary basic knowledge and assumptions are reviewed.

A. DYNAMIC MODEL

The high-speed train is formalized by the multi-particle model, in which each car is regarded as a mass point and the entire train is composed of multiple mass points connected through the couplers. By Newton's law, a widely used dynamic motion model from [11] with respect to each car is presented as follows,

$$\begin{cases} \dot{s}_j(t) = v_j(t), \\ m_j(t)\dot{v}_j(t) = u_j(t) + f_j^b(t, v_j(t)) \\ \qquad\qquad + f_j^c(t, \boldsymbol{s}(t), \boldsymbol{v}(t)) + f_j^a(t), \end{cases} \tag{1}$$

where $j \in \{1, 2, \ldots, n\}$ is the index of cars, $t \in [0, T]$ represents the operation period of train, $s_j(t)$ and $v_j(t)$ denote the displacement and velocity of the jth car respectively, $m_j(t)$ is the mass of the jth car, $u_j(t)$ denotes the traction force or braking force according to the sign of $u_j(t)$, $f_j^b(\cdot)$, $f_j^c(\cdot)$ and $f_j^a(\cdot)$ represent respectively the basic resistance, coupler force and additional resistance suffered by the jth car. Concretely, the expressions of basic resistance and coupler force can be established,

$$f_j^b(t, v_j(t)) = \begin{cases} -m_j(t)\left[c_0(t) + c_v(t)v_j(t)\right] \\ \qquad - \sum_{k=1}^{n} m_k(t)c_a(t)v_1^2(t), & j = 1, \\ -m_j(t)\left[c_0(t) + c_v(t)v_j(t)\right], & j = 2, \ldots, n. \end{cases} \tag{2}$$

$$f_j^c(t, \boldsymbol{s}(t), \boldsymbol{v}(t)) = \begin{cases} -c_k(t)[s_1(t) - s_2(t)] - c_d(t)[v_1(t) - v_2(t)], \\ \qquad\qquad j = 1, \\ c_k(t)[s_{j-1}(t) - s_j(t)] + c_d(t)[v_{j-1}(t) - v_j(t)] \\ \quad - c_k(t)[s_j(t) - s_{j+1}(t)] - c_d(t)[v_j(t) \\ \quad - v_{j+1}(t)], \qquad j = 2, \ldots, n-1, \\ c_k(t)[s_{n-1}(t) - s_n(t)] + c_d(t)[v_{n-1}(t) \\ \quad - v_n(t)], \qquad j = n. \end{cases} \tag{3}$$

It can be seen from (2) that the basic resistance $f_j^b(\cdot)$ consists of two parts, namely the mechanical resistance $m_j(t)[c_0(t) + c_v(t)v_j(t)]$ and the aerodynamic resistance $\sum_{k=1}^{n} m_k(t)c_a(t)v_1^2(t)$. (3) demonstrates that the coupler resistance $f_j^c(\cdot)$ mainly comes from the front car ($c_k(t)[s_{j-1}(t) - s_j(t)] + c_d(t)[v_{j-1}(t) - v_j(t)]$) and rear car ($c_k(t)[s_j(t) - s_{j+1}(t)] + c_d(t)[v_j(t) - v_{j+1}(t)]$), due to the deviation of displacement or velocity between the adjacent cars. $c_0(t)$, $c_v(t)$, $c_a(t)$, $c_k(t)$ and $c_d(t)$ are the related resistance coefficients, which are defined as unknown state-independent time-varying parameters. Moreover, since the additional resistance $f_j^a(\cdot)$ is generally caused by the infrastructures, e.g., slopes, tunnels, bridges, etc., it is considered as the unknown state-independent continuous function.

To facilitate the presentation, some arguments of functions and time-varying parameters are dropped without arising confusion, e.g., $f_j^b(v_j)$, f_j^a, c_0, etc.

Normally, to reduce the physical loss of actuator, the control inputs are artificially restrained by a soft limiter. Let μ_j denote the unsaturated control input calculated directly by controller, and u_j represent the actual input of control system shown in (1). For motor cars and trailers respectively, the saturation operators of input are defined as follows.

When the jth car belongs to the motor cars,

$$u_j = \mathrm{sat}(\mu_j, u_j^-, u_j^+) = \begin{cases} u_j^+, & \mu_j > u_j^+, \\ \mu_j, & u_j^- \le \mu_j \le u_j^+, \\ u_j^-, & \mu_j < u_j^-. \end{cases} \tag{4}$$

When the jth car belongs to the trailers,

$$u_j = \mathrm{sat}(\mu_j, u_j^-, 0) = \begin{cases} 0, & \mu_j > 0, \\ \mu_j, & u_j^- \le \mu_j \le 0, \\ u_j^-, & \mu_j < u_j^-. \end{cases} \tag{5}$$

u_j^+ denotes the maximal traction force of the jth motor car, u_j^- is the maximal braking force of the jth car, both of which are known constants.

For the saturation operators, there exists the following property.

Property 1 ([38]): For $\underline{g}, g, \overline{g} \in \mathbb{R}$ satisfying $\underline{g} \leq g \leq \overline{g}$, then the following inequality holds,

$$[(\gamma + 1)g - (\gamma h + \mathrm{sat}(g, \underline{g}, \overline{g}))][h - \mathrm{sat}(h, \underline{g}, \overline{g})] \leq 0, \tag{6}$$

where $h = \mathrm{sat}(g, \underline{g}, \overline{g})$ and $\gamma \geq 0$.

Furthermore, an assumption on the mass of cars $m_j(t)$ is specified as follows.

Assumption 1: The unknown time-varying parameter $m_j(t)$ has the known lower bound $\underline{m}_j$ and upper bound $\overline{m}_j$, i.e., $\underline{m}_j \leq m_j(t) \leq \overline{m}_j$, where $\underline{m}_j, \overline{m}_j$ are constants, and $\underline{m}_j > 0$.

Remark 1: Assumption 1 is reasonable when $\underline{m}_j$ represents the self-weight of jth car, and $\overline{m}_j$ denotes the mass of jth car with full load.

B. PROBLEM FORMULATION

The idea of ILC is to utilize the tracking error and control input information in the previous operation to enhance the tracking control performance of current operation, when the control task of trains is repeatable and periodic. Hence, let $s_{i,j}$, $v_{i,j}$ and $u_{i,j}$ denote the displacement, velocity and input of the jth car at the ith operation respectively, whose vector forms are defined as $\boldsymbol{s}_i, \boldsymbol{v}_i, \boldsymbol{u}_i \in \mathbb{R}^{n\times 1}$ with respect to the entire train. From (1), (2) and (3), the dynamic model of train is rewritten as

$$\begin{cases} \dot{\boldsymbol{s}}_i = \boldsymbol{v}_i, \\ M\dot{\boldsymbol{v}}_i = \boldsymbol{u}_i + \Theta_v \boldsymbol{v}_i + \theta_a \phi(\boldsymbol{v}_i) + \theta_k A \boldsymbol{s}_i + \theta_d A \boldsymbol{v}_i + \boldsymbol{\eta}, \end{cases} \tag{7}$$

where

$$M(t) = \mathcal{D}(m_1, m_2, \ldots, m_n) \in \mathbb{R}^{n\times n},$$
$$\Theta_v(t) = \mathcal{D}(-c_v m_1, -c_v m_2, \ldots, -c_v m_n) \in \mathbb{R}^{n\times n},$$
$$\theta_a(t) = -c_a \sum_{k=1}^{n} m_k \in \mathbb{R},$$
$$\phi(\boldsymbol{v}_i) = \left[v_{i,1}^2, 0, \ldots, 0\right]_n^T \in \mathbb{R}^{n\times 1},$$
$$\theta_k(t) = -c_k \in \mathbb{R}, \quad \theta_d(t) = -c_d \in \mathbb{R},$$
$$A = \begin{bmatrix} 1 & -1 & 0 & 0 & \cdots \\ -1 & 2 & -1 & 0 & \cdots \\ \vdots & \vdots & \ddots & \vdots & \vdots \\ 0 & \cdots & -1 & 2 & -1 \\ 0 & \cdots & 0 & -1 & 1 \end{bmatrix} \in \mathbb{R}^{n\times n},$$
$$\boldsymbol{\eta}(t) = \left[f_1^a - c_0 m_1, f_2^a - c_0 m_2, \ldots, f_n^a - c_0 m_n\right]^T \in \mathbb{R}^{n\times 1}.$$

The unknown time-varying parametric terms M, Θ_v, θ_a, θ_k, θ_d and $\boldsymbol{\eta}$ will be estimated in our controller. Moreover, the lower and upper bounds of M are defined as $\underline{M} = \mathcal{D}(\underline{m}_1, \underline{m}_2, \ldots, \underline{m}_n)$ and $\overline{M} = \mathcal{D}(\overline{m}_1, \overline{m}_2, \ldots, \overline{m}_n)$ according to *Assumption* 1.

Similarly, the distributed input constraints (4) and (5) could also be unified as the following vector form,

$$\boldsymbol{u}_i = \mathrm{sat}(\boldsymbol{\mu}_i, \underline{\boldsymbol{u}}, \overline{\boldsymbol{u}}), \tag{8}$$

where $\underline{\boldsymbol{u}} = [u_1^-, u_2^-, \ldots, u_n^-]^T \in \mathbb{R}^{n\times 1}$, the elements of $\overline{\boldsymbol{u}} \in \mathbb{R}^{n\times 1}$ will be u_j^+ or 0 depending on the distribution of power systems.

The objective of this paper is to devise the tracking controller to drive the trains to follow the given reference displacement $\boldsymbol{s}_r(t) = [s_r(t), s_r(t), \ldots, s_r(t)]_n^T \in \mathbb{R}^{n\times 1}$ and velocity $\boldsymbol{v}_r(t) = [v_r(t), v_r(t), \ldots, v_r(t)]_n^T \in \mathbb{R}^{n\times 1}$, that $\dot{\boldsymbol{s}}_r(t) = \boldsymbol{v}_r(t)$ obviously.

To attain the objective of control, some reasonable assumptions on the control system (7) and reference trajectories are required.

Assumption 2: There is always an appropriate control input $\boldsymbol{u}_r(t)$ to drive the high-speed train to track the reference trajectories $\boldsymbol{s}_r$ and $\boldsymbol{v}_r$ over the finite time interval $[0, T]$.

Remark 2: Assumption 2 guarantees that the train system should be controllable, especially in the presence of the input constraints.

Assumption 3: The initial states of all cars are identical with the initial values of reference trajectories at every iteration, i.e., $\boldsymbol{s}_i(0) = \boldsymbol{s}_r(0)$ and $\boldsymbol{v}_i(0) = \boldsymbol{v}_r(0)$.

Remark 3: The identical initialization condition (i.i.c) or its modifications are essential for the stability analysis of control system, which can be easily satisfied in the repetitive operation environment of high-speed trains.

Remark 4: At present, although some ILC schemes have been presented to deal with the tracking control of high-speed train, there are still many issues that need to be solved. Concretely, the existing learning controllers in [28]–[31], [36], and [37] are designed based on the single-particle model which belongs to a class of first-order single input single output system. Since the single-particle model cannot distinguish the control input of each car, it is impossible to explore the influence of distributed input constraints on the entire train as the multi-particle model does. Therefore, it is highly significant to integrate the ILC method and the second-order multi-particle model of train. Recently, [35] proposed an ILC scheme for high-order system by using the backstepping technique, where the input saturation is handled through introducing an auxiliary system. Motivated by these works, an adaptive ILC strategy is constructed in this paper to achieve the tracking control of displacement and velocity for high-speed train in the presence of distributed input constraints.

III. CONTROLLER DESIGN AND ANALYSIS

In this section, the ILC controller is devised to achieve the tracking of reference trajectories for high-speed trains with the help of the backstepping design procedure. To ensure the control performance, an input-dependent auxiliary system is established to compensate the influence of input constraints. Finally, the stability of control system and the convergence of tracking errors are confirmed by constructing CEF.

The auxiliary system for input constraints is defined as follows,

$$\begin{cases} \dot{\boldsymbol{\lambda}}_{1,i} = -c_1 \boldsymbol{\lambda}_{1,i} + \boldsymbol{\lambda}_{2,i}, \\ \dot{\boldsymbol{\lambda}}_{2,i} = -c_2 \boldsymbol{\lambda}_{2,i} + c_3 \Delta \boldsymbol{u}_i, \end{cases} \tag{9}$$

where c_1, c_2 and c_3 are all the designed positive constants, $\Delta \boldsymbol{u}_i = \boldsymbol{u}_i - \boldsymbol{\mu}_i$ represents the difference between the actual input of control system and the unsaturated input calculated by controller. It could be found that $\boldsymbol{\lambda}_{1,i} \in \mathbb{R}^{n\times 1}$ and $\boldsymbol{\lambda}_{2,i} \in \mathbb{R}^{n\times 1}$ remain zero when there is no saturation to occur, i.e., $\Delta \boldsymbol{u}_i = 0$, otherwise nonzero.

Following the procedure of backstepping technique, the coordinate transformation of closed-loop system involving (7) and (9) is established,

$$\begin{aligned} z_{1,i} &= \boldsymbol{s}_i - \boldsymbol{s}_r - \boldsymbol{\lambda}_{1,i}, \\ z_{2,i} &= \boldsymbol{v}_i - \boldsymbol{v}_r - \boldsymbol{\alpha}_i - \boldsymbol{\lambda}_{2,i}, \end{aligned} \tag{10}$$

where $\boldsymbol{\alpha}_i$ is the virtual controller.

The design of ILC controller is performed in two steps, where the virtual controller is devised at the first step, and the real controller is constructed at the second step.

Step 1: Taking the derivative of $z_{1,i}$ and combining (9) and (10), it has

$$\begin{aligned} \dot{z}_{1,i} &= \boldsymbol{v}_i - \boldsymbol{v}_r - \boldsymbol{\lambda}_{2,i} + c_1\boldsymbol{\lambda}_{1,i} \\ &= z_{2,i} + \boldsymbol{\alpha}_i + c_1\boldsymbol{\lambda}_{1,i}. \end{aligned} \tag{11}$$

One selects the following virtual controller,

$$\boldsymbol{\alpha}_i = -c_1(\boldsymbol{s}_i - \boldsymbol{s}_r). \tag{12}$$

Defining the Lyapunov function $V_{1,i} = \frac{1}{2}\left\|z_{1,i}\right\|^2$, the derivative of which considering (11) and (12) is given as follows,

$$\dot{V}_{1,i} = -c_1\left\|z_{1,i}\right\|^2 + z_{1,i}^T z_{2,i}. \tag{13}$$

Step 2: By taking the derivative of $z_{2,i}$ and combining (7) and (9), it can be obtained

$$\begin{aligned} \dot{z}_{2,i} &= c_3\left(\boldsymbol{u}_i + \Theta_3\boldsymbol{v}_i + \theta_a\phi(\boldsymbol{v}_i) + \theta_k A\boldsymbol{s}_i + \theta_d A\boldsymbol{v}_i \right.\\ &\quad \left. + \boldsymbol{\eta}\right) - c_3 M\dot{\boldsymbol{v}}_i + \dot{\boldsymbol{v}}_i - \dot{\boldsymbol{v}}_r - \dot{\boldsymbol{\alpha}}_i + c_2\boldsymbol{\lambda}_{2,i} \\ &\quad - c_3\Delta\boldsymbol{u}_i \\ &= c_3\boldsymbol{\mu}_i + c_3\left(\Theta_v\boldsymbol{v}_i + \theta_a\phi(\boldsymbol{v}_i) + \theta_k A\boldsymbol{s}_i \right.\\ &\quad \left. + \theta_d A\boldsymbol{v}_i + \boldsymbol{\eta} - M\dot{\boldsymbol{v}}_i\right) + \dot{\boldsymbol{v}}_i - \dot{\boldsymbol{v}}_r - \dot{\boldsymbol{\alpha}}_i \\ &\quad + c_2\boldsymbol{\lambda}_{2,i}. \end{aligned} \tag{14}$$

Defining the Lyapunov function $V_{2,i} = \frac{1}{2}\left\|z_{2,i}\right\|^2$, one gets its derivative in terms of (14) as follows,

$$\begin{aligned} \dot{V}_{2,i} &= z_{2,i}^T\left[c_3\boldsymbol{\mu}_i + c_3\left(\Theta_v\boldsymbol{v}_i + \theta_a\phi(\boldsymbol{v}_i) + \theta_k A\boldsymbol{s}_i \right.\right.\\ &\quad \left. + \theta_d A\boldsymbol{v}_i + \boldsymbol{\eta} - M\dot{\boldsymbol{v}}_i\right) + \dot{\boldsymbol{v}}_i - \dot{\boldsymbol{v}}_r - \dot{\boldsymbol{\alpha}}_i \\ &\quad \left. + c_2\boldsymbol{\lambda}_{2,i}\right] \\ &= z_{2,i}^T\left[c_3\boldsymbol{\mu}_i + c_3\left(\hat{\Theta}_{v,i}\boldsymbol{v}_i + \hat{\theta}_{a,i}\phi(\boldsymbol{v}_i) \right.\right.\\ &\quad \left. + \hat{\theta}_{k,i}A\boldsymbol{s}_i + \hat{\theta}_{d,i}A\boldsymbol{v}_i + \hat{\boldsymbol{\eta}}_i - \hat{M}_i\dot{\boldsymbol{v}}_i\right) + \dot{\boldsymbol{v}}_i \\ &\quad \left. - \dot{\boldsymbol{v}}_r - \dot{\boldsymbol{\alpha}}_i + c_2\boldsymbol{\lambda}_{2,i}\right] - c_3 z_{2,i}^T\tilde{\Theta}_{v,i}\boldsymbol{v}_i \\ &\quad - c_3 z_{2,i}^T\tilde{\theta}_{a,i}\phi(\boldsymbol{v}_i) - c_3 z_{2,i}^T\tilde{\theta}_{k,i}A\boldsymbol{s}_i \\ &\quad - c_3 z_{2,i}^T\tilde{\theta}_{d,i}A\boldsymbol{v}_i - c_3 z_{2,i}^T\tilde{\boldsymbol{\eta}}_i + c_3 z_{2,i}^T\tilde{M}_i\dot{\boldsymbol{v}}_i, \end{aligned} \tag{15}$$

where $\hat{\Theta}_{v,i}$ is the estimation of Θ_v at the ith iteration, $\tilde{\Theta}_{v,i} = \hat{\Theta}_{v,i} - \Theta_v$ is the estimation error, $\hat{\theta}_{a,i}$, $\tilde{\theta}_{a,i}$, $\hat{\theta}_{k,i}$, $\tilde{\theta}_{k,i}$, $\hat{\theta}_{d,i}$, $\tilde{\theta}_{d,i}$, $\hat{\boldsymbol{\eta}}_i$, $\tilde{\boldsymbol{\eta}}_i$, $\hat{M}_i$ and $\tilde{M}_i$ are defined similarly.

The following control law of ILC scheme at ith iteration is constructed,

$$\begin{aligned} \boldsymbol{\mu}_i &= -\frac{1}{c_3}\left[c_2\left(\boldsymbol{v}_i - \boldsymbol{v}_r - \boldsymbol{\alpha}_i\right) + \dot{\boldsymbol{v}}_i - \dot{\boldsymbol{v}}_r - \dot{\boldsymbol{\alpha}}_i + z_{1,i}\right] \\ &\quad - \left(\hat{\Theta}_{v,i}\boldsymbol{v}_i + \hat{\theta}_{a,i}\phi(\boldsymbol{v}_i) + \hat{\theta}_{k,i}A\boldsymbol{s}_i + \hat{\theta}_{d,i}A\boldsymbol{v}_i \right.\\ &\quad \left. + \hat{\boldsymbol{\eta}}_i - \hat{M}_i\dot{\boldsymbol{v}}_i\right), \\ \boldsymbol{u}_i &= \text{sat}\left(\boldsymbol{\mu}_i, \underline{\boldsymbol{u}}, \overline{\boldsymbol{u}}\right). \end{aligned} \tag{16}$$

Accordingly, the parameters learning rules at ith iteration is proposed as follows,

$$\hat{\Theta}_{v,i} = \hat{\Theta}_{v,i-1} + \gamma_v \cdot c_3 \cdot \mathcal{D}(z_{2,i}) \cdot \mathcal{D}(\boldsymbol{v}_i), \quad \hat{\Theta}_{v,0} = 0, \tag{17}$$

$$\hat{\theta}_{a,i} = \hat{\theta}_{a,i-1} + \gamma_a \cdot c_3 \cdot z_{2,i}^T\phi(\boldsymbol{v}_i), \quad \hat{\theta}_{a,0} = 0, \tag{18}$$

$$\hat{\theta}_{k,i} = \hat{\theta}_{k,i-1} + \gamma_k \cdot c_3 \cdot z_{2,i}^T A\boldsymbol{s}_i, \quad \hat{\theta}_{k,0} = 0, \tag{19}$$

$$\hat{\theta}_{d,i} = \hat{\theta}_{d,i-1} + \gamma_d \cdot c_3 \cdot z_{2,i}^T A\boldsymbol{v}_i, \quad \hat{\theta}_{d,0} = 0, \tag{20}$$

$$\hat{\boldsymbol{\eta}}_i = \hat{\boldsymbol{\eta}}_{i-1} + \gamma_\eta \cdot c_3 \cdot z_{2,i}, \quad \hat{\boldsymbol{\eta}}_0 = 0, \tag{21}$$

$$\begin{aligned} \hat{M}_i &= \text{sat}\left(\hat{M}_{i-1} - \gamma_M \cdot c_3 \cdot \mathcal{D}(z_{2,i}) \cdot \mathcal{D}(\dot{\boldsymbol{v}}_i), \underline{M}, \overline{M}\right), \\ \hat{M}_0 &= \underline{M}, \end{aligned} \tag{22}$$

where γ_v, γ_a, γ_k, γ_d, γ_η and γ_M are the parametric learning gain, which are all positive constants. On account of *Assumption* 1, the saturation operator is applied to the learning process of M to retain its estimation within the required bounds.

Consider $z_{1,i}$ and $z_{2,i}$ together, the Lyapunov function for the closed-loop control system at ith iteration is written as

$$V_i = V_{1,i} + V_{2,i}. \tag{23}$$

According to (13), (15) and (16), the derivative of V_i is

$$\begin{aligned} \dot{V}_i &= -c_1\left\|z_{1,i}\right\|^2 - c_2\left\|z_{2,i}\right\|^2 - c_3 z_{2,i}^T\tilde{\Theta}_{v,i}\boldsymbol{v}_i \\ &\quad - c_3 z_{2,i}^T\tilde{\theta}_{a,i}\phi(\boldsymbol{v}_i) - c_3 z_{2,i}^T\tilde{\theta}_{k,i}A\boldsymbol{s}_i \\ &\quad - c_3 z_{2,i}^T\tilde{\theta}_{d,i}A\boldsymbol{v}_i - c_3 z_{2,i}^T\tilde{\boldsymbol{\eta}}_i + c_3 z_{2,i}^T\tilde{M}_i\dot{\boldsymbol{v}}_i. \end{aligned} \tag{24}$$

Theorem 1: For the control system (7) of high-speed trains with distributed input constraints (8) satisfying *Assumption* 2, 3 and 1, the control law (16) and the parameter learning rules (17)-(22) can guarantee that,

1) All variables are bounded.

2) $z_{1,i}$ and $z_{2,i}$ converge to 0 along the iteration axis.

3) The tracking errors $\boldsymbol{s}_i - \boldsymbol{s}_r$ and $\boldsymbol{v}_i - \boldsymbol{v}_r$ will remain within the compact bounds, namely,

$$\begin{cases} \int_0^T \|\boldsymbol{s}_i - \boldsymbol{s}_r\|^2 d\tau \le \dfrac{2}{c_z}E_{i-1} + \dfrac{c_3}{c_\lambda}\int_0^T \|\Delta\boldsymbol{u}_i\|^2 d\tau, \\ \int_0^T \|\boldsymbol{v}_i - \boldsymbol{v}_r\|^2 d\tau \le \dfrac{2}{c_z}E_{i-1} + \dfrac{c_3}{c_\lambda}\int_0^T \|\Delta\boldsymbol{u}_i\|^2 d\tau, \end{cases}$$

where the parameters c_z and c_λ will be defined later.

Proof: To prove the stability of control system and the convergence of tracking errors, one established the following

CEF at the ith iteration,

$$\begin{aligned}E_i &= V_i + \frac{1}{2\gamma_v}\int_0^t \mathrm{tr}(\tilde{\Theta}_{v,i}^2)d\tau + \frac{1}{2\gamma_a}\int_0^t \tilde{\theta}_{a,i}^2 d\tau \\ &+ \frac{1}{2\gamma_k}\int_0^t \tilde{\theta}_{k,i}^2 d\tau + \frac{1}{2\gamma_d}\int_0^t \tilde{\theta}_{d,i}^2 d\tau \\ &+ \frac{1}{2\gamma_\eta}\int_0^t \left\|\tilde{\boldsymbol{\eta}}_i\right\|^2 d\tau + \frac{1}{2\gamma_M}\int_0^t \mathrm{tr}(\tilde{M}_i^2)d\tau. \quad (25)\end{aligned}$$

The whole proof is composed of three parts.

Step 1 (Non-Increasing of CEF):

To analyze the changes of CEF along the iteration axis, the difference of CEF is defined as follows,

$$\begin{aligned}\Delta E_i &= E_i - E_{i-1} \\ &= V_i - V_{i-1} + \frac{1}{2\gamma_v}\int_0^t \mathrm{tr}\left(\tilde{\Theta}_{v,i}^2 - \tilde{\Theta}_{v,i-1}^2\right) d\tau \\ &+ \frac{1}{2\gamma_a}\int_0^t \left(\tilde{\theta}_{a,i}^2 - \tilde{\theta}_{a,i-1}^2\right) d\tau + \frac{1}{2\gamma_k}\int_0^t \left(\tilde{\theta}_{k,i}^2 \right.\\ &\left. - \tilde{\theta}_{k,i-1}^2\right) d\tau + \frac{1}{2\gamma_d}\int_0^t \left(\tilde{\theta}_{d,i}^2 - \tilde{\theta}_{d,i-1}^2\right) d\tau \\ &+ \frac{1}{2\gamma_\eta}\int_0^t \left(\left\|\tilde{\boldsymbol{\eta}}_i\right\|^2 - \left\|\tilde{\boldsymbol{\eta}}_{i-1}\right\|^2\right) d\tau + \frac{1}{2\gamma_M} \\ &\int_0^t \mathrm{tr}\left(\tilde{M}_i^2 - \tilde{M}_{i-1}^2\right) d\tau. \quad (26)\end{aligned}$$

The third term on the right side of (26) through invoking the parameter learning rule (17) can be derived as,

$$\begin{aligned}&\frac{1}{2\gamma_v}\int_0^t \mathrm{tr}\left(\tilde{\Theta}_{v,i}^2 - \tilde{\Theta}_{v,i-1}^2\right) d\tau \\ &= \frac{1}{2\gamma_v}\int_0^t \mathrm{tr}\left((\hat{\Theta}_{v,i-1} - \hat{\Theta}_{v,i})(2\Theta_v - \hat{\Theta}_{v,i} - \hat{\Theta}_{v,i-1})\right) d\tau \\ &= \frac{1}{\gamma_v}\int_0^t \mathrm{tr}\left((\hat{\Theta}_{v,i} - \hat{\Theta}_{v,i-1})\tilde{\Theta}_{v,i}\right) d\tau \\ &\quad - \frac{1}{2\gamma_v}\int_0^t \mathrm{tr}\left((\hat{\Theta}_{v,i-1} - \hat{\Theta}_{v,i})^2\right) d\tau \\ &\le c_3\int_0^t z_{2,i}^T\tilde{\Theta}_{v,i}\boldsymbol{v}_i d\tau. \quad (27)\end{aligned}$$

Similarly, according to (18)-(21), it has the following results,

$$\frac{1}{2\gamma_a}\int_0^t \left(\tilde{\theta}_{a,i}^2 - \tilde{\theta}_{a,i-1}^2\right) d\tau \le c_3\int_0^t z_{2,i}^T\phi(\boldsymbol{v}_i)\tilde{\theta}_{a,i} d\tau, \quad (28)$$

$$\frac{1}{2\gamma_k}\int_0^t \left(\tilde{\theta}_{k,i}^2 - \tilde{\theta}_{k,i-1}^2\right) d\tau \le c_3\int_0^t z_{2,i}^T A s_i\tilde{\theta}_{k,i} d\tau, \quad (29)$$

$$\frac{1}{2\gamma_d}\int_0^t \left(\tilde{\theta}_{d,i}^2 - \tilde{\theta}_{d,i-1}^2\right) d\tau \le c_3\int_0^t z_{2,i}^T A\boldsymbol{v}_i\tilde{\theta}_{d,i} d\tau, \quad (30)$$

$$\frac{1}{2\gamma_\eta}\int_0^t \left(\left\|\tilde{\boldsymbol{\eta}}_i\right\|^2 - \left\|\tilde{\boldsymbol{\eta}}_{i-1}\right\|^2\right) d\tau \le c_3\int_0^t z_{2,i}^T\tilde{\boldsymbol{\eta}}_i d\tau. \quad (31)$$

Noticing the parameter learning rule (22), one handles the sixth term on the right side of (26) as follows,

$$\begin{aligned}&\frac{1}{2\gamma_M}\int_0^t \mathrm{tr}\left(\tilde{M}_i^2 - \tilde{M}_{i-1}^2\right) d\tau \\ &\le \frac{1}{\gamma_M}\int_0^t \mathrm{tr}\left((\hat{M}_{i-1} - \hat{M}_i)(M - \hat{M}_i)\right) d\tau \\ &= \frac{1}{\gamma_M}\int_0^t \mathrm{tr}\left((\hat{M}_{i-1} - \gamma_M \cdot c_3 \cdot \mathcal{D}(z_{2,i}) \cdot \mathcal{D}(\dot{\boldsymbol{v}}_i) - \hat{M}_i)\right.\\ &\quad \left.(M - \mathrm{sat}(\hat{M}_{i-1} - \gamma_M \cdot c_3 \cdot \mathcal{D}(z_{2,i}) \cdot \mathcal{D}(\dot{\boldsymbol{v}}_i), \underline{M}, \overline{M}))\right) d\tau \\ &\quad - c_3\int_0^t \mathrm{tr}\left(\mathcal{D}(z_{2,i}) \cdot \mathcal{D}(\dot{\boldsymbol{v}}_i) \cdot \tilde{M}_i\right) d\tau. \quad (32)\end{aligned}$$

Using *Property* 1 and letting $\gamma = 0$, one can obtain

$$\begin{aligned}&\mathrm{tr}\left((\hat{M}_{i-1} - \gamma_M \cdot c_3 \cdot \mathcal{D}(z_{2,i}) \cdot \mathcal{D}(\dot{\boldsymbol{v}}_i) - \hat{M}_i)\right.\\ &\left.(M - \mathrm{sat}(\hat{M}_{i-1} - \gamma_M \cdot c_3 \cdot \mathcal{D}(z_{2,i}) \cdot \mathcal{D}(\dot{\boldsymbol{v}}_i), \underline{M}, \overline{M}))\right) \le 0. \quad (33)\end{aligned}$$

Substituting (33) into (32), it yields

$$\frac{1}{2\gamma_M}\int_0^t \mathrm{tr}\left(\tilde{M}_i^2 - \tilde{M}_{i-1}^2\right) d\tau \le -c_3\int_0^t z_{2,i}^T\tilde{M}_i\dot{\boldsymbol{v}}_i d\tau. \quad (34)$$

According to the facts of $V_{i-1}(t) \ge 0$ and $V_i(t) = \int_0^t \dot{V}_i(\tau)d\tau$ indicated by *Assumption* 3, substituting (24), (27)-(31) and (34) into (26) yields

$$\Delta E_i \le -c_1\int_0^t \left\|z_{1,i}\right\|^2 d\tau - c_2\int_0^t \left\|z_{2,i}\right\|^2 d\tau \le 0. \quad (35)$$

Now, the non-increasing of CEF along the iteration axis is verified.

Step 2: (Convergence of Tracking Error)

Before proving the convergence of tracking error, the boundedness of CEF should be confirmed. On account of the non-increasing of CEF, it is only required to prove that $E_1(t)$ is bounded.

In terms of (24) and (25) with $i = 1$, the derivative of E_1 can be obtained

$$\begin{aligned}\dot{E}_1 &= -c_3 z_{2,i}^T\tilde{\Theta}_{v,1}\boldsymbol{v}_1 + \frac{1}{2\gamma_v}\mathrm{tr}\left(\tilde{\Theta}_{v,1}^2\right) \\ &- c_3 z_{2,1}^T\tilde{\theta}_{a,1}\phi(\boldsymbol{v}_1) + \frac{1}{\gamma_a}\tilde{\theta}_{a,1}^2 - c_3 z_{2,1}^T\tilde{\theta}_{k,1}A s_1 \\ &+ \frac{1}{2\gamma_k}\tilde{\theta}_{k,1}^2 - c_3 z_{2,1}^T\tilde{\theta}_{d,1}A\boldsymbol{v}_1 + \frac{1}{2\gamma_d}\tilde{\theta}_{d,1}^2 \\ &- c_3 z_{2,1}^T\tilde{\boldsymbol{\eta}}_1 + \frac{1}{2\gamma_\eta}\left\|\tilde{\boldsymbol{\eta}}_1\right\|^2 + c_3 z_{2,1}\tilde{M}_1\dot{\boldsymbol{v}}_1 \\ &+ \frac{1}{2\gamma_M}\mathrm{tr}\left(\tilde{M}_1^2\right). \quad (36)\end{aligned}$$

Owning to (17) with $i = 0$, i.e., $\hat{\Theta}_{v,0} = 0$, rewriting the first term term and second term on the right side of (36) leads to that

$$\begin{aligned}&-c_3 z_{2,1}^T\tilde{\Theta}_{v,1}\boldsymbol{v}_1 + \frac{1}{2\gamma_v}\mathrm{tr}\left(\tilde{\Theta}_{v,1}^2\right) \\ &= -c_3 z_{2,1}^T\tilde{\Theta}_{v,1}\boldsymbol{v}_1 + \frac{1}{2\gamma_v}\mathrm{tr}\left(\tilde{\Theta}_{v,1}^2 - \tilde{\Theta}_{v,0}^2\right) \\ &+ \frac{1}{2\gamma_v}\mathrm{tr}\left(\Theta_v^2\right). \quad (37)\end{aligned}$$

Recalling (27), it is obvious that

$$\frac{1}{2\gamma_v}\mathrm{tr}\left(\tilde{\Theta}_{v,1}^2 - \tilde{\Theta}_{v,0}^2\right) \le c_3 z_{2,1}^T\tilde{\Theta}_{v,1}\boldsymbol{v}_1. \quad (38)$$

Using (38), (37) becomes

$$-c_3 z_{2,1}^T \tilde{\Theta}_{v,1} \boldsymbol{v}_1 + \frac{1}{2\gamma_v} \mathrm{tr}\left(\tilde{\Theta}_{v,1}^2\right) \leq \frac{1}{2\gamma_v} \mathrm{tr}\left(\Theta_v^2\right). \tag{39}$$

Similarly, it has

$$-c_3 z_{2,1}^T \tilde{\theta}_{a,1} \phi(\boldsymbol{v}_1) + \frac{1}{2\gamma_a} \tilde{\theta}_{a,1}^2 \leq \frac{1}{2\gamma_a} \theta_a^2, \tag{40}$$

$$-c_3 z_{2,1}^T \tilde{\theta}_{k,1} A \boldsymbol{s}_1 + \frac{1}{2\gamma_k} \tilde{\theta}_{k,1}^2 \leq \frac{1}{2\gamma_k} \theta_k^2, \tag{41}$$

$$-c_3 z_{2,1}^T \tilde{\theta}_{d,1} A \boldsymbol{v}_1 + \frac{1}{2\gamma_d} \tilde{\theta}_{d,1}^2 \leq \frac{1}{2\gamma_d} \theta_d^2, \tag{42}$$

$$-c_3 z_{2,1}^T \tilde{\boldsymbol{\eta}}_1 + \frac{1}{2\gamma_\eta} \left\|\tilde{\boldsymbol{\eta}}_1\right\|^2 \leq \frac{1}{2\gamma_\eta} \|\boldsymbol{\eta}\|^2, \tag{43}$$

$$c_3 z_{2,1}^T \tilde{M}_1 \dot{\boldsymbol{v}}_1 + \frac{1}{2\gamma_M} \mathrm{tr}\left(\tilde{M}_1^2\right) \leq \frac{1}{2\gamma_M} \mathrm{tr}\left((\underline{M} - M)^2\right). \tag{44}$$

Substituting (39)-(44) into (36) yields

$$\dot{E}_1 \leq \frac{1}{2} \mathrm{tr}\left(\Theta_v^2\right) + \frac{1}{2\gamma_a} \theta_a^2 + \frac{1}{2\gamma_k} \theta_k^2 + \frac{1}{2\gamma_d} \theta_d^2 + \frac{1}{2\gamma_\eta} \|\boldsymbol{\eta}\|^2 + \frac{1}{2\gamma_M} \mathrm{tr}\left((\underline{M} - M)^2\right). \tag{45}$$

It can draw conclusion from (45) that E_1 is bounded in the finite interval $[0, T]$ since the right side of (45) is a continuous iteration-independent function.

Considering (35), the following inequality on the CEF can be obtained immediately,

$$E_i \leq E_1 - c_1 \sum_{k=2}^{i} \int_0^t \left\|z_{1,k}\right\|^2 d\tau - c_2 \sum_{k=2}^{i} \int_0^t \left\|z_{2,k}\right\|^2 d\tau. \tag{46}$$

Taking the limitation on the both sides of (46), it leads to that

$$\lim_{i \to +\infty} E_i = E_1 - c_1 \cdot \lim_{i \to +\infty} \sum_{k=2}^{i} \int_0^t \left\|z_{1,k}\right\|^2 d\tau - c_2 \cdot \lim_{i \to +\infty} \sum_{k=2}^{i} \int_0^t \left\|z_{2,k}\right\|^2 d\tau. \tag{47}$$

Since E_i is nonnegative and bounded, according to the limit theorem, it is easy to obtain that

$$\begin{cases} \lim_{i \to \infty} \int_0^t \left\|z_{1,i}\right\|^2 d\tau = 0, \\ \lim_{i \to \infty} \int_0^t \left\|z_{2,i}\right\|^2 d\tau = 0. \end{cases} \tag{48}$$

Defining the Lyapunov function $V_{\lambda,i} = \frac{1}{2}\left\|\boldsymbol{\lambda}_{1,i}\right\|^2 + \frac{1}{2}\left\|\boldsymbol{\lambda}_{2,i}\right\|^2$ for the auxiliary system, its derivative is derived by using the Young's inequality and (9) as follows,

$$\begin{aligned} \dot{V}_{\lambda,i} &= -c_1 \left\|\boldsymbol{\lambda}_{1,i}\right\|^2 + \boldsymbol{\lambda}_{1,i}^T \boldsymbol{\lambda}_{2,i} - c_2 \left\|\boldsymbol{\lambda}_{2,i}\right\|^2 + c_3 \boldsymbol{\lambda}_{2,i}^T \Delta \boldsymbol{u}_i \\ &\leq -(c_1 + \frac{1}{2}) \left\|\boldsymbol{\lambda}_{1,i}\right\|^2 - (c_2 - \frac{1}{2} - \frac{c_3}{2}) \left\|\boldsymbol{\lambda}_{2,i}\right\|^2 + \frac{c_3}{2} \left\|\Delta \boldsymbol{u}_i\right\|^2 \\ &\leq -c_\lambda (\left\|\boldsymbol{\lambda}_{1,i}\right\|^2 + \left\|\boldsymbol{\lambda}_{2,i}\right\|^2) + \frac{c_3}{2} \left\|\Delta \boldsymbol{u}_i\right\|^2, \end{aligned} \tag{49}$$

where $c_\lambda = \min(c_1 - \frac{1}{2}, c_2 - \frac{1}{2} - \frac{c_3}{2})$ is a positive constant. Integrating both side of (49), it gets that

$$V_{\lambda,i}(T) - V_{\lambda,i}(0) \leq -c_\lambda \int_0^T (\left\|\boldsymbol{\lambda}_{1,i}\right\|^2 + \left\|\boldsymbol{\lambda}_{2,i}\right\|^2) d\tau + \frac{c_3}{2} \int_0^T \left\|\Delta \boldsymbol{u}_i\right\|^2 d\tau. \tag{50}$$

Considering the fact of $V_{\lambda,i}(0) = 0$ and $V_{\lambda,i}(T) \geq 0$, one has

$$\int_0^T (\left\|\boldsymbol{\lambda}_{1,i}\right\|^2 + \left\|\boldsymbol{\lambda}_{2,i}\right\|^2) d\tau \leq \frac{c_3}{2c_\lambda} \int_0^T \left\|\Delta \boldsymbol{u}_i\right\|^2 d\tau. \tag{51}$$

Recalling (35), it follows that

$$\int_0^T (\left\|z_{1,i}\right\|^2 + \left\|z_{2,i}\right\|^2) d\tau \leq \frac{1}{c_z}(E_{i-1} - E_i) \leq \frac{1}{c_z} E_{i-1}. \tag{52}$$

where $c_z = \min(c_1, c_2)$. Defining the tracking errors $\boldsymbol{e}_{s,i} = \boldsymbol{s}_i - \boldsymbol{s}_r$, $\boldsymbol{e}_{v,i} = \boldsymbol{v}_i - \boldsymbol{v}_r$ and considering (10), the following inequality holds,

$$\begin{aligned} &\int_0^T \left[(1 + c_1) \left\|\boldsymbol{e}_{s,i}\right\|^2 + \left\|\boldsymbol{e}_{v,i}\right\|^2\right] d\tau \\ &\leq 2 \int_0^T (\left\|z_{1,i}\right\|^2 + \left\|z_{2,i}\right\|^2) d\tau + 2 \int_0^T (\left\|\boldsymbol{\lambda}_{1,i}\right\|^2 + \left\|\boldsymbol{\lambda}_{2,i}\right\|^2) d\tau. \end{aligned} \tag{53}$$

From (51), (52) and (53), it easily leads to

$$\int_0^T \left\|\boldsymbol{e}_{s,i}\right\|^2 d\tau \leq \frac{2}{c_z} E_{i-1} + \frac{c_3}{c_\lambda} \int_0^T \left\|\Delta \boldsymbol{u}_i\right\|^2 d\tau, \tag{54}$$

and

$$\int_0^T \left\|\boldsymbol{e}_{v,i}\right\|^2 d\tau \leq \frac{2}{c_z} E_{i-1} + \frac{c_3}{c_\lambda} \int_0^T \left\|\Delta \boldsymbol{u}_i\right\|^2 d\tau. \tag{55}$$

Hence, it can conclude that the tracking errors are bounded by (54) and (55) with the designed parameters c_λ and c_z, as well as $z_{1,i}$ and $z_{2,i}$ are convergent along the iteration axis point-wisely.

Step 3 (Boundedness of Variables):

The boundedness of E_i, $z_{1,i}$, $z_{2,i}$ and the tracking errors have been proved in the last steps. According the definition of E_i, it can draw the conclusion that $\Theta_{v,i}$, $\theta_{a,i}$, $\theta_{k,i}$, $\theta_{d,i}$, $\boldsymbol{\eta}_i$ and M_i are all bounded. Moreover, since $\boldsymbol{s}_r$ and $\boldsymbol{v}_r$ are the known bounded variables in the interval $[0, T]$, the displacement $\boldsymbol{s}_i$ and velocity $\boldsymbol{v}_i$ are also bounded in $[0, T]$ according to (54) and (55). ■

Remark 5: Since the difference between actual input and unsaturated input $\Delta \boldsymbol{u}_i$ is integrated to z_i via the auxiliary system, the design of controller is allowed to be carried out through following the standard backstepping procedure. Nevertheless, it should be noted that the designed errors z_1 is different from the common tracking error $\boldsymbol{s}_i - \boldsymbol{s}_r$ in the general backstepping control scheme. Therefore, when constructing the controller, we usually choose the appropriate parameters c_1, c_2, c_3 to mitigate the influence of input constraints on the tracking error. Furthermore, it should be emphasized that $\boldsymbol{\lambda}_{1,i}$ and $\boldsymbol{\lambda}_{2,i}$ gradually decay to zero after the end of input constraints, i.e., the auxiliary system will be non-activation.

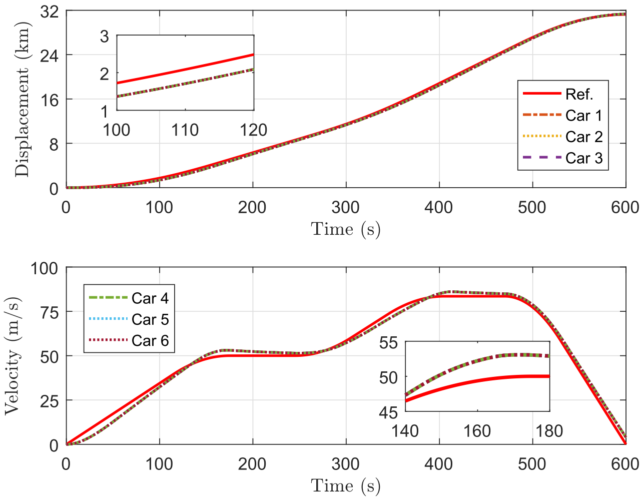

FIGURE 1. The tracking profiles of displacement and velocity at the first iteration.

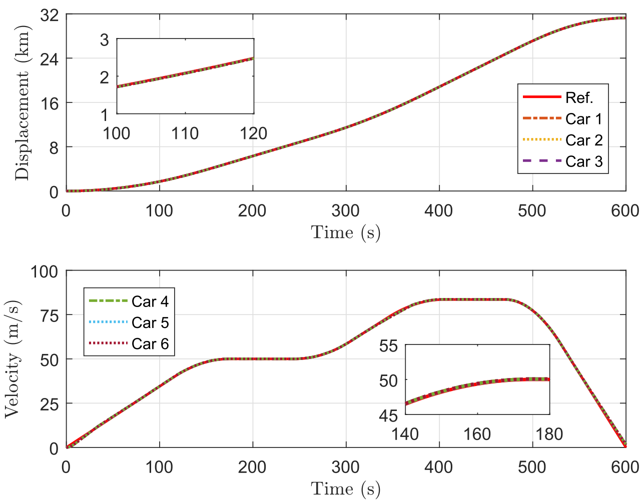

FIGURE 2. The tracking profiles of displacement and velocity at the 30th iteration.

TABLE 1. The simulation parameters for CRH3 [13].

Parameter	Value	Unit
$m_1, m_2, \cdots, m_6$	5×10^4	kg
c_0	7.75×10^{-3}	N/kg
c_v	2.28×10^{-4}	N·s/(m·kg)
c_a	1.66×10^{-5}	N·s^2/(m^2·kg)
c_k	2×10^6	N/m
c_d	1×10^5	N·s/m

IV. SIMULATION AND DISCUSSION

Numerical simulation is performed to analyze the effectiveness of proposed ILC scheme for high-speed trains with distributed input constraints, including the tracking control performance of velocity and displacement, as well as the influence of the limitations of power systems on the control input signals. The parameters for simulation are from the CRH3 train, which are listed in TABLE 1.

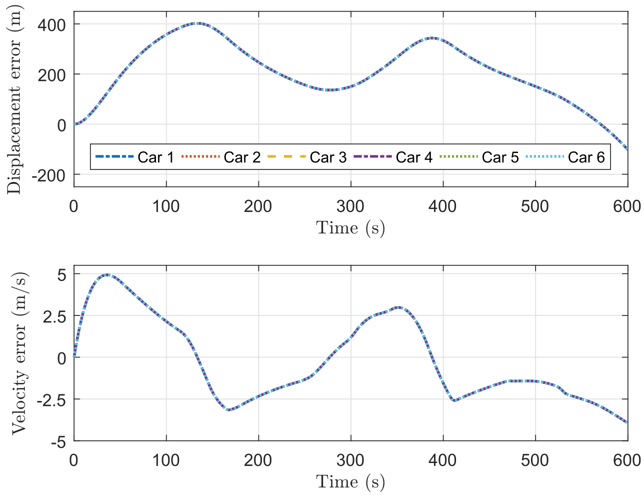

FIGURE 3. The tracking error profiles of displacement and velocity at the first iteration.

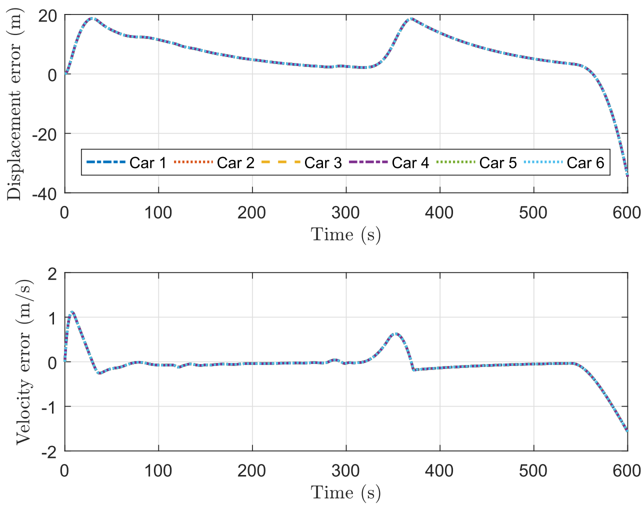

FIGURE 4. The tracking error profiles of displacement and velocity at the 30th iteration.

The given reference trajectory covers the three scenarios of acceleration, cruise, and deceleration for the train operation, the details of which will be shown in the simulation results later. In the accelerating phase, the power systems of the motor cars provide the traction forces, to drag or push the trailers via the coupler forces from the adjacent cars, thus driving the train to speed up. In the decelerating phase, the braking systems of motor cars and trailers works simultaneously to slow the train down until stop. The simulated train is composed of six cars in our paper, where the distribution of motor cars is 101010, that is, the 1st car, the 3th car and the 5th car are motor cars, the others are trailers. Further, the maximum traction force and maximum braking force are assigned as 4×10^4 N, i.e., $\underline{u} = [-4, -4, \ldots, -4]^T \times 10^4$ and $\overline{u} = [4, 0, 4, 0, 4, 0]^T \times 10^4$. Moreover, 83.5 m/s (approximately 300 km/h) is considered as the final cruising velocity.

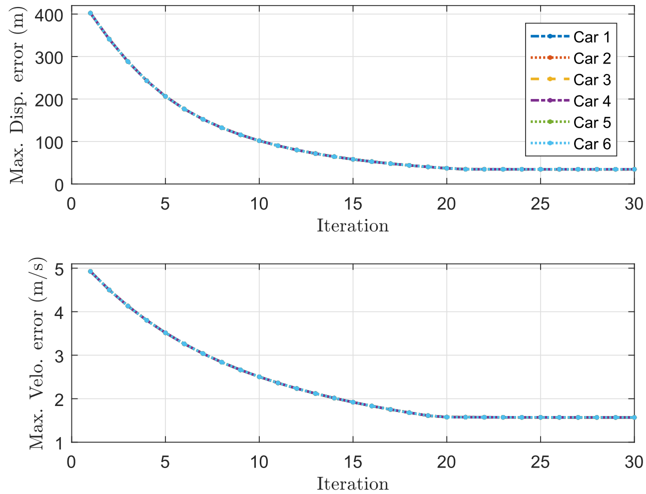

FIGURE 5. The maximum tracking errors of displacement and velocity versus the iteration number.

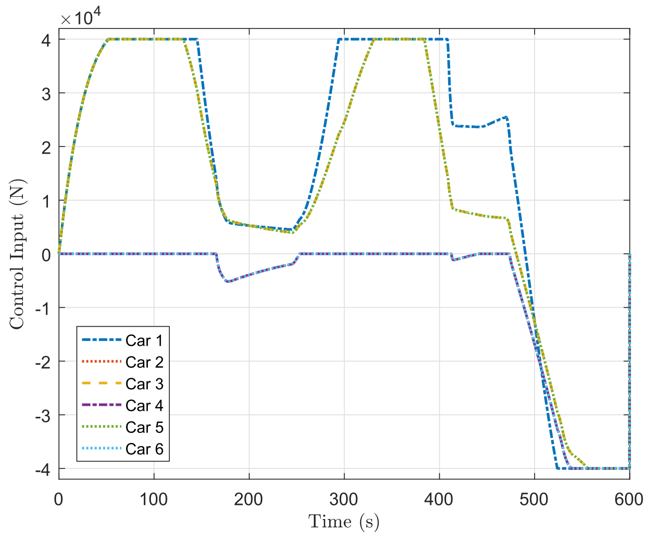

FIGURE 6. The profiles of control input subjected to constraints at the first iteration (u_1).

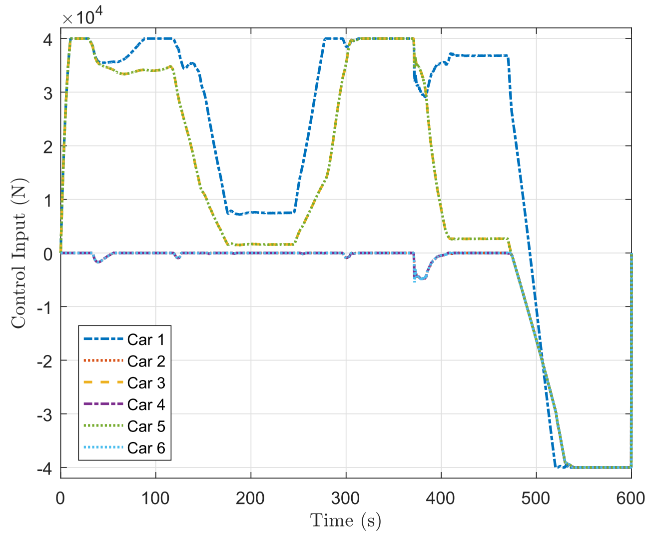

FIGURE 7. The profiles of control input subjected to constraints at the 30th iteration (u_{30}).

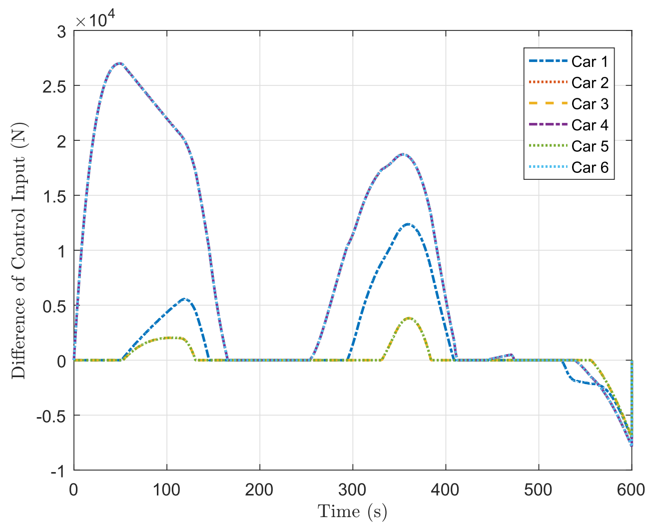

FIGURE 8. The profiles of difference between the actual control input and the unsaturated input at the first iteration ($\Delta u_1 = u_1 - \mu_1$).

According to the requirements with respect to the stability of control system and the learning efficiency of ILC, we set the controller parameters as $c_1 = 0.01, c_2 = 100, c_3 = 0.04$, the learning gains as $\gamma_v = 10, \gamma_a = 0.02, \gamma_k = \gamma_d = \gamma_\eta = \gamma_M = 8000$, where the selection of values takes fully into account the convergence speed of tracking errors and the possible magnitude of estimated parameters. Following the procedure developed in Section III, and applying the designed parameters, the control input at the ith operation of train is constructed as follows,

$$\begin{aligned} \boldsymbol{u}_i = \operatorname{sat}\big(&-25 \times [100 \times (\boldsymbol{v}_i - \boldsymbol{v}_r + 0.01 \times \boldsymbol{s}_i - 0.01 \times \boldsymbol{s}_r) \\ &+ \dot{\boldsymbol{v}}_i - \dot{\boldsymbol{v}}_r + 0.01 \times \boldsymbol{v}_i - 0.01 \times \boldsymbol{v}_r + \boldsymbol{s}_i - \boldsymbol{s}_r - \boldsymbol{\lambda}_{1,i}] \\ &- (\hat{\Theta}_{v,i}\boldsymbol{v}_i + \hat{\theta}_{a,i}\phi(\boldsymbol{v}_i) + \hat{\theta}_{k,i}A\boldsymbol{s}_i + \hat{\theta}_{d,i}A\boldsymbol{v}_i + \hat{\boldsymbol{\eta}}_i \\ &- \hat{M}_i\dot{\boldsymbol{v}}_i), \underline{\boldsymbol{u}}, \overline{\boldsymbol{u}}\big), \end{aligned}$$

and the estimation of unknown parameters at the ith iteration can be calculated as,

$$\begin{aligned} \hat{\Theta}_{v,i} &= \hat{\Theta}_{v,i-1} + 0.4 \times \mathcal{D}(z_{2,i}) \cdot \mathcal{D}(\boldsymbol{v}_i), \\ \hat{\theta}_{a,i} &= \hat{\theta}_{a,i-1} + 0.0008 \times z_{2,i}^T \phi(\boldsymbol{v}_i), \\ \hat{\theta}_{k,i} &= \hat{\theta}_{k,i-1} + 320 \times z_{2,i}^T A\boldsymbol{s}_i, \\ \hat{\theta}_{d,i} &= \hat{\theta}_{d,i-1} + 320 \times z_{2,i}^T A\boldsymbol{v}_i, \\ \hat{\boldsymbol{\eta}}_i &= \hat{\boldsymbol{\eta}}_{i-1} + 320 \times z_{2,i}, \\ \hat{M}_i &= \operatorname{sat}\left(\hat{M}_{i-1} - 320 \times \mathcal{D}(z_{2,i}) \cdot \mathcal{D}(\dot{\boldsymbol{v}}_i), \underline{M}, \overline{M}\right). \end{aligned}$$

30 iterations are executed to ensure the tracking of reference trajectories for high-speed trains, as well as to discuss the variation of the control input constraints. More details are given as follows.

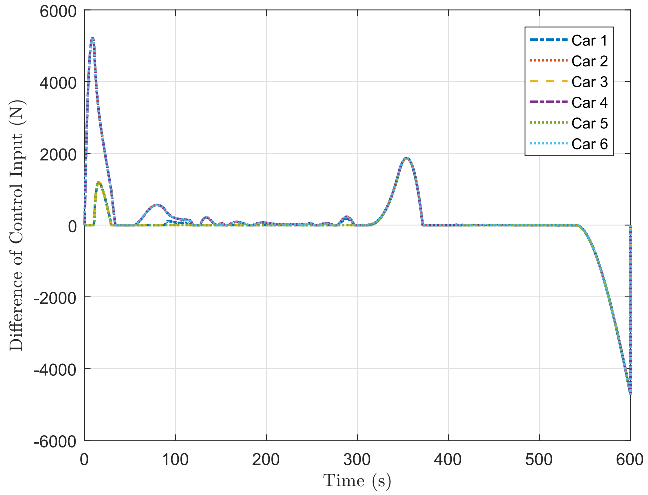

FIGURE 9. The profiles of difference between the actual control input and the unsaturated input at the 30th iteration ($\Delta u_{30} = u_{30} - \mu_{30}$).

Figs. 1 and 2 demonstrate the tracking profiles of displacement and velocity of all cars at the first iteration and 30th iteration, respectively. It can be seen from Fig. 1 that there are significant deviations between the actual measured displacements/velocities of cars and the given reference displacements/velocities. Obviously, although there is also the adaptive term in the controller during the first iteration, it is intractable to achieve the better tracking results in the finite time interval due to the irregular changes of reference trajectories. Nevertheless, as shown in Fig. 2, the effect of tracking control is significantly enhanced at the 30 iteration since the estimations of unknown parameters are adjusted between successive operations via iteration learning.

Concretely, the tracking errors of displacement and velocity are shown in Figs. 3 and 4 respectively, and the maximum absolute errors at each iteration are given in Fig. 5, both of which not only quantitatively verify the effect of parameters learning, but also illustrate the asymptotic convergence of tracking errors. Although the maximum tracking errors of velocity at the 30th iteration in Fig. 5 have not been eliminated completely, the errors are closely remained around zero at the most period of entire operation as shown in Fig. 4, and the tracking errors of displacement are similar. Moreover, theoretically, the tracking errors could be further converged if there are more iterations to be executed without the consideration of simulation cost. Overall, Figs. 1 to 5 confirm the tracking control performance of the proposed ILC scheme for high-speed trains.

To indicate that the distributed input constraints are indeed abode, the control forces of all cars at the first iteration and 30th iteration are exhibited in Figs. 6 and 7. It shows that, during the entire process of each operation, the traction forces are only provided by the motor cars, i.e., Car 1, 3, 5, and the braking forces come from all the motor cars and trailers. Further, to observe the influence of iteration learning on the input signals, the differences between the actual control forces of train and the unsaturated inputs at the first iteration and 30th iteration are given in Figs. 8 and 9 respectively. It could be found that the input signals calculated directly by the controller at the 30th iteration are closer to the scope specified by the input constraints than the first iteration. That is, with the development of iterations, the proposed ILC scheme is helpful to improve the input signals of controller according to the requirements of the distribution and output capacity of power systems.

V. CONCLUSION

In this paper, an adaptive ILC scheme is constructed to achieve the tracking control of displacement and velocity for high-speed trains in the presence of distributed input constraints, where the multi-particle model is employed to describe the dynamics of train. To devise the learning controller, an auxiliary system is established to overcome the input saturation, and the backstepping design procedure is used to derive the control law (16) and parameters learning rules (17)-(22). Moreover, the stability of control systems and the convergence of tracking errors are proved via constructing CEF, as well as the effectiveness of proposed scheme is verified by numerical simulation.

REFERENCES

[1] H.-S. Hwang, "Control strategy for optimal compromise between trip time and energy consumption in a high-speed railway," *IEEE Trans. Syst., Man, Cybern. A, Syst., Humans*, vol. 28, no. 6, pp. 791–802, Nov. 1998.
[2] Y. Song and W. Song, "A novel dual speed-curve optimization based approach for energy-saving operation of high-speed trains," *IEEE Trans. Intell. Transp. Syst.*, vol. 17, no. 6, pp. 1564–1575, Jun. 2016.
[3] S. Li, L. Yang, Z. Gao, and K. Li, "Optimal guaranteed cost cruise control for high-speed train movement," *IEEE Trans. Intell. Transp. Syst.*, vol. 17, no. 10, pp. 2879–2887, Oct. 2016.
[4] M. Faieghi, A. Jalali, and S. K. M. Mashhadi, "Robust adaptive cruise control of high speed trains," *ISA Trans.*, vol. 53, no. 2, pp. 533–541, Mar. 2014.
[5] H. Tang, Q. Wang, and X. Feng, "Robust stochastic control for high-speed trains with nonlinearity, parametric uncertainty, and multiple time-varying delays," *IEEE Trans. Intell. Transp. Syst.*, vol. 19, no. 4, pp. 1027–1037, Apr. 2018.
[6] X. Yao, J. H. Park, H. Dong, L. Guo, and X. Lin, "Robust adaptive nonsingular terminal sliding mode control for automatic train operation," *IEEE Trans. Syst., Man, Cybern., Syst.*, to be published.
[7] M. Faieghi, A. Jalali, S. K.-E.-D. M. Mashhadi, and D. Baleanu, "Passivity-based cruise control of high speed trains," *J. Vib. Control*, vol. 24, no. 3, pp. 492–504, 2018.
[8] S. Li, L. Yang, K. Li, and Z. Gao, "Robust sampled-data cruise control scheduling of high speed train," *Transp. Res. C, Emerg. Technol.*, vol. 46, no. 46, pp. 274–283, 2014.
[9] L. Shukai, Y. Lixing, and L. Ke-Ping, "Robust output feedback cruise control for high-speed train movement with uncertain parameters," *Chin. Phys. B*, vol. 24, no. 1, 2014, Art. no. 010503.
[10] H. Tang, X. Lin, X. Ge, and Q. Wang, "Hierarchical multi-mode high-speed train speed controller based on H_∞," in *Proc. IEEE 18th Int. Conf. Intell. Transp. Syst.*, 2015, pp. 1817–1824.
[11] T. Tao and H. Xu, "Adaptive fault-tolerant cruise control for a class of high-speed trains with unknown actuator failure and control input saturation," *Math. Problems Eng.*, vol. 2014, Jun. 2014, Art. no. 481315.
[12] X. Guo, J. Zhao, and W. Xiao, "CNN-based adaptive tracking control for high speed train with asymmetric input saturation," in *Proc. 8th Int. Conf. Intell. Control Inf. Process. (ICICIP)*, Nov. 2017, pp. 129–134.
[13] Y. Yang, Z. Xu, W. Liu, H. Li, R. Zhang, and Z. Huang, "Optimal operation of high-speed trains using hybrid model predictive control," *J. Adv. Transp.*, vol. 2018, Apr. 2018, Art. no. 7308058.

[14] S. Gao, H. Dong, Y. Chen, B. Ning, and G. Chen, "Adaptive and robust automatic train control systems with input saturation," *Control Intell. Syst.*, vol. 41, no. 2, pp. 103–111, 2013.

[15] X. Lin, H. Dong, X. Yao, and W. Bai, "Neural adaptive fault-tolerant control for high-speed trains with input saturation and unknown disturbance," *Neurocomputing*, vol. 260, pp. 32–42, Oct. 2017.

[16] S. Li, L. Yang, and Z. Gao, "Adaptive coordinated control of multiple high-speed trains with input saturation," *Nonlinear Dyn.*, vol. 83, no. 4, pp. 2157–2169, 2016.

[17] D. Huang, X. Li, W. He, and S. Zhang, "Iterative learning control for boundary tracking of uncertain nonlinear wave equations," *J. Franklin Inst.*, vol. 355, no. 17, pp. 8441–8461, 2018.

[18] Y. Chen, T. Meng, Y. Wang, K. Wang, S. Meng, and D. Huang, "Iterative learning control of two-phase laminar flow interface in Y-shaped microfluidic channel," *IEEE Trans. Control Syst. Technol.*, to be published.

[19] Y. Jian, D. Huang, J. Liu, and D. Min, "High-precision tracking of piezoelectric actuator using iterative learning control and direct inverse compensation of hysteresis," *IEEE Trans. Ind. Electron.*, vol. 66, no. 1, pp. 368–377, Jan. 2019.

[20] D. Shen and J.-X. Xu, "Adaptive learning control for nonlinear systems with randomly varying iteration lengths," *IEEE Trans. Neural Netw. Learn. Syst.*, vol. 30, no. 4, pp. 1119–1132, Apr. 2019.

[21] D. Shen, "Data-driven learning control for stochastic nonlinear systems: Multiple communication constraints and limited storage," *IEEE Trans. Neural Netw. Learn. Syst.*, vol. 29, no. 6, pp. 2429–2440, Jun. 2018.

[22] D. Shen and J.-X. Xu, "Distributed learning consensus for heterogenous high-order nonlinear multi-agent systems with output constraints," *Automatica*, vol. 97, pp. 64–72, Nov. 2018.

[23] D. Shen and J.-X. Xu, "A novel Markov chain based ILC analysis for linear stochastic systems under general data dropouts environments," *IEEE Trans. Autom. Control*, vol. 62, no. 11, pp. 5850–5857, Nov. 2017.

[24] C.-S. Teo, K.-K. Tan, and S.-Y. Lim, "Dynamic geometric compensation for gantry stage using iterative learning control," *IEEE Trans. Instrum. Meas.*, vol. 57, no. 2, pp. 413–419, Feb. 2008.

[25] R.-E. Precup, S. Preitl, I. J. Rudas, M. L. Tomescu, and J. K. Tar, "Design and experiments for a class of fuzzy controlled servo systems," *IEEE/ASME Trans. Mechatronics*, vol. 13, no. 1, pp. 22–35, Feb. 2008.

[26] X. Lu, H. Chen, B. Gao, Z. Zhang, and W. Jin, "Data-driven predictive gearshift control for dual-clutch transmissions and FPGA implementation," *IEEE Trans. Ind. Electron.*, vol. 62, no. 1, pp. 599–610, Jan. 2015.

[27] D. Shen, J. Han, and Y. Wang, "Convergence analysis of ILC input sequence for underdetermined linear systems," *Sci. China Inf. Sci.*, vol. 60, no. 9, 2017, Art. no. 099201.

[28] Y. Wang, Z. Hou, and X. Li, "A novel automatic train operation algorithm based on iterative learning control theory," in *Proc. IEEE Int. Conf. Service Oper. Logistics, Informat.*, vol. 2, Oct. 2008, pp. 1766–1770.

[29] Z. Li, Z. Hou, and C. Yin, "Iterative learning control for train trajectory tracking under speed constrains with iteration-varying parameter," *Trans. Inst. Meas. Control*, vol. 37, no. 4, pp. 485–493, Apr. 2014.

[30] Z. Hou, Y. Wang, C. Yin, and T. Tong, "Terminal iterative learning control based station stop control of a train," *Int. J. Control*, vol. 84, no. 7, pp. 1263–1274, 2011.

[31] H. Q. Sun, Z. S. Hou, and D. Y. Li, "Coordinated iterative learning control schemes for train trajectory tracking with overspeed protection," *IEEE Trans. Autom. Sci. Eng.*, vol. 10, no. 2, pp. 323–333, Apr. 2013.

[32] J.-X. Xu, Y. Tan, and T.-H. Lee, "Iterative learning control design based on composite energy function with input saturation," *Automatica*, vol. 40, no. 8, pp. 1371–1377, 2004.

[33] H. Ji, Z. Hou, L. Fan, and F. L. Lewis, "Adaptive iterative learning reliable control for a class of non-linearly parameterised systems with unknown state delays and input saturation," *IET Control Theory Appl.*, vol. 10, no. 17, pp. 2160–2174, Nov. 2016.

[34] Q. Yu, Z. Hou, and R. Chi, "Adaptive iterative learning control for nonlinear uncertain systems with both state and input constraints," *J. Franklin Inst.*, vol. 353, no. 15, pp. 3920–3943, Oct. 2016.

[35] H. Benslimane, A. Boulkroune, and H. Chekireb, "Adaptive iterative learning control of nonlinearly parameterised strict feedback systems with input saturation," *Int. J. Autom. Control*, vol. 12, no. 2, pp. 251–270, 2018.

[36] L. Fan, "Iterative learning and adaptive fault-tolerant control with application to high-speed trains under unknown speed delays and control input saturations," *IET Control Theory Appl.*, vol. 8, no. 9, pp. 675–687, Jun. 2014.

[37] H. Ji, Z. Hou, and R. Zhang, "Adaptive iterative learning control for high-speed trains with unknown speed delays and input saturations," *IEEE Trans. Autom. Sci. Eng.*, vol. 13, no. 1, pp. 260–273, Jan. 2016.

[38] M. Sun and S. S. Ge, "Adaptive repetitive control for a class of nonlinearly parametrized systems," *IEEE Trans. Autom. Control*, vol. 51, no. 10, pp. 1684–1688, Oct. 2006.

YONG CHEN received the M.S. degree from the School of Computer and Software Engineering, Xihua University, Chengdu, China, in 2016. He is currently pursuing the Ph.D. degree with the School of Electrical Engineering, Southwest Jiaotong University, Chengdu. His research interests include iterative learning control, microfluidics, and operation control of high-speed trains.

DEQING HUANG received the B.S. and Ph.D. degrees in applied mathematics from the Mathematical College, Sichuan University, Chengdu, China, in 2002 and 2007, respectively, and the Ph.D. degree in control engineering from the Department of Electrical and Computer Engineering (ECE), National University of Singapore (NUS), Singapore, in 2011. He attended ECE, NUS, in 2006. From 2010 to 2013, he was a Research Fellow with the Department of Electrical and Computer Engineering, NUS. From 2013 to 2016, he was a Research Associate with the Department of Aeronautics, Imperial College London, London, U.K. In 2016, he joined the Department of Electronic and Information Engineering, Southwest Jiaotong University, Chengdu, China, as a Professor and the Department Head. His research interests include modern control theory, artificial intelligence, and fault diagnosis and robotics.

TENGFEI HUANG was born in China, in 1992. He received the B.S. degree in electronic and information engineering from Southwest Jiaotong University, Chengdu, China, in 2016, where he is currently pursuing the M.S. degree. His research interests include iterative learning control of high-speed trains and energy efficient driving.

NA QIN received the M.S. and Ph.D. degrees in power system and automation from the School of Electrical Engineering, Southwest Jiaotong University, Chengdu, China, in 2003 and 2014, respectively, where she is currently an Associate Professor. Her research interests include intelligent information processing, artificial intelligence, iterative learning control, and fault diagnosis.